International Conference on Space Optics—ICSO 2022

Dubrovnik, Croatia

3–7 October 2022

Edited by Kyriaki Minoglou, Nikos Karafolas, and Bruno Cugny,

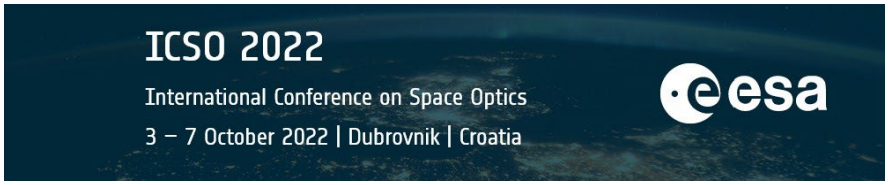

Realizing an all-glass beam splitter for space by using advanced joining technologies

International Conference on Space Optics — ICSO 2022, edited by Kyriaki Minoglou, Nikos Karafolas, Bruno Cugny, Proc. of SPIE Vol. 12777, 1277719 · © 2023 ESA and CNES · 0277-786X · doi: 10.1117/12.2689276

Realizing an all-glass beam splitter for space by using advanced joining technologies

Carolin Rothhardt[a], Pascal Birckigt[a,b], Kevin Grabowski[a], Stefan Risse[a], Ralph Schlegel[a], Svetlana Shestaeva[a], Stefan Schwinde[a], Sebastian Schmidl[c], and Sylvio Klose[c]

[a]Fraunhofer Institute for Applied Optics and Precision Engineering, Albert-Einstein Straße 7, 07745 Jena, Germany
[b]Institute of Applied Physics, Max-Wien-Platz 1, 07743 Jena, Germany
[c]Thüringer Landessternwarte Tautenburg, Sternwarte 5, 07778 Tautenburg, Germany

ABSTRACT

Joining technologies are of great importance for space-based applications. Given the very low environmental temperatures, high temperature differences, vacuum, and high acceleration loads during rocket launch, the (thermo-)mechanical requirements on the joining technologies are demanding. Plasma-activated bonding (PAB) and silicate bonding (SB) meet all these requirements. We developed PAB and SB to assemble an all-glass four-channel beam splitter. This development was initiated by a satellite mission concept, devoted to transient astronomy. Central part of this satellite mission is a novel beam splitter that divides the incoming telescope beam into four near infrared channels ($\lambda = 800 - 1700$ nm), by using a Kösters prism type design. As a final result, we built a demonstrator for the validation of the developed technological concept.

Keywords: direct bonding, silicate bonding, coating, beam splitter, dielectric coating

1. INTRODUCTION

The cubesat mission SkyHopper[1] aims at hunting exploding stars. The photons of these cosmologically distant targets, are shifted to the red on their way to the observer. The most distant objects in the remote universe cannot be detected in the visible spectral range anymore, but in the near infrared (NIR). Atmospheric absorptions and emission strongly affect ground-based NIR observations. The space-based detection of distant exploding stars avoids atmospheric perturbations. For this application, four equally wide channels within a spectral range of $\lambda = 800 - 1700$ nm need to be observed simultaneously. To save volume and mass within a cubesat, a single detector is used to detect the four spectral channels. A Kösters type prism[2,3] is an elegant solution to realize this beam splitter. Here, three beam splitting prism pairs separate the incoming light from a telescope into four channels.

In this paper we present the results of setting up an all-glass beam splitter, shown schematically in fig. 1. All prisms consist of fused silica (Infrasil). The incoming beam in fig. 1 represents the image coming from a telescope (field of view 1.76° x 0.44°; pupil diameter 224 mm). An anti-reflective (AR) coating reduces losses on the entrance face of prism D. The first beam splitter separates the incoming beam into shorter wavelengths ($\lambda = 800$ - 1150 nm) and longer wavelengths ($\lambda = 1150$ - 1700 nm). A long-pass filter on prism C and a short-pass filter on prism D further filters the beams. The dichroic beam splitting coating, labelled "2" splits the longer wavelength beams into two channels ($\lambda = 1150$ - 1400 nm according to the astronomic "J" band and $\lambda = 1400$ - 1700 nm according to the astronomic "H" band). Total reflection on the interface of the prisms A and B to vacuum steer the beams onto the detector (Hawaii-2RG, operating temperature 140 K). In the same way, the short wavelength beam is separated into two beams (950 - 1150 nm, according to the astronomic "z" band and $\lambda = 800$ - 950 nm, according to the astronomic "Y" band). Besides their optical functionality, the three beam splitter coatings also serve as interface for bonding the two prisms. We used plasma-activated bonding (PAB) to prevent optical losses, which is presented in detail in section 3. To realize the necessary vacuum gaps for the total reflection, the prisms are mounted onto a glass plate by silicate bonding (SB), as presented in section 4.

Further author information: (Send correspondence to C.R.)
C.R.: E-mail: carolin.rothhardt@iof.fraunhofer.de, Telephone: +49 3641 807 304

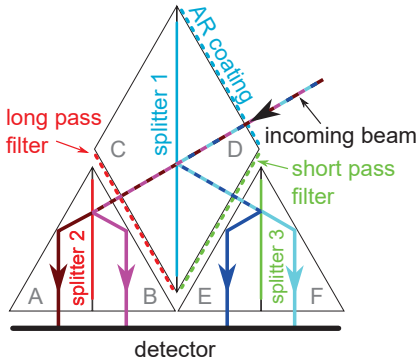

Figure 1. Scheme of the beamsplitter assembly. The incoming beam is divided into two beams by the first beam splitter coating. Each of the split beams is again split into two beams by the beam splitters "2" and "3", as specified in table 1. An anti-reflective coating reduces losses on the entrance plane. Long-pass and short-pass filters on the exit faces of prism C and D filter unwanted light.

2. COATING

Table 1 summarizes the optical specifications of the different coatings. At the same time, the coating surfaces provide an interface for direct bonding of the prism pairs (A with B, C with D, and E with F as shown in fig. 1). The AR coating and the filter coatings are necessary to meet the high requirements on the optical performance of the whole beam splitter setup.[4] A ternary design of the coating system is used to keep the overall coating thickness at 4 µm. SiO_2 serves as low-index material and silicon as high-index material for the beam splitter coating systems. Si_3N_4 and Ta_2O_5 were evaluated as medium-index material. Details on the evaluation of their optical properties can be found here.[4] A final SiO_2 layer was included in the coating design, which provides the interface for the bonding.

Table 1. Specifications of the coatings applied on the beam splitter.

Coating	Transmitting range	Reflecting or blocking range	Angle of Incidence (AOI)
Dichroic beam splitter 1	1150 - 1700 nm	reflecting range: 800 - 1150 nm	30°
Dichroic beam splitter 2	1400 - 1700 nm	reflecting range: 1150 - 1400 nm	30°
Dichroic beam splitter 3	950 - 1150 nm	reflecting range: 800 - 950 nm	30°
Anti-reflective coating	800 - 1700 nm		0°
Short-pass filter		blocking range: 1150 - 1700 nm	0°
Long pass filter		blocking range: 800 - 1150 nm	0°

3. DIRECT BONDING

Standard beam splitter cubes are joined with index-matching adhesives. Adhesives consist of polymers, which are prone to outgassing and ageing in harsh conditions like space. Here we present our results to use PAB for the joining of beam splitter coatings in space. PAB is established within semiconductor processes for some decades.[5] Recently, various optical components were bonded successfully for different applications, like frequency conversion with nonlinear crystals in high power laser systems[6] or prism-grating-prism assemblies for use in space-based spectrometers.[7]

3.1 Surface Characterization

For plasma-activated bonding a direct connection between the surfaces is established without any auxiliary material. To bring the surface atoms into close contact, the sample's surfaces need to be smooth (root mean

square roughness, σ_{rms} <1 nm in a 100 µm² measurement area), flat (surface flatness better $\lambda/4$ for stiff samples with $\lambda = 633$ nm) and very clean.[5] Applying 4 µm thick coatings results in high surface roughness above 1 nm rms (fig. 2, left). Hence, we used a ~200 nm thick SiO_2 layer as top layer of the dichroic beam splitter coating systems. This SiO_2 top layer is chemical mechanical polished (CMP) to achieve the necessary low roughness (even below 0.3 nm rms, fig. 2, right).

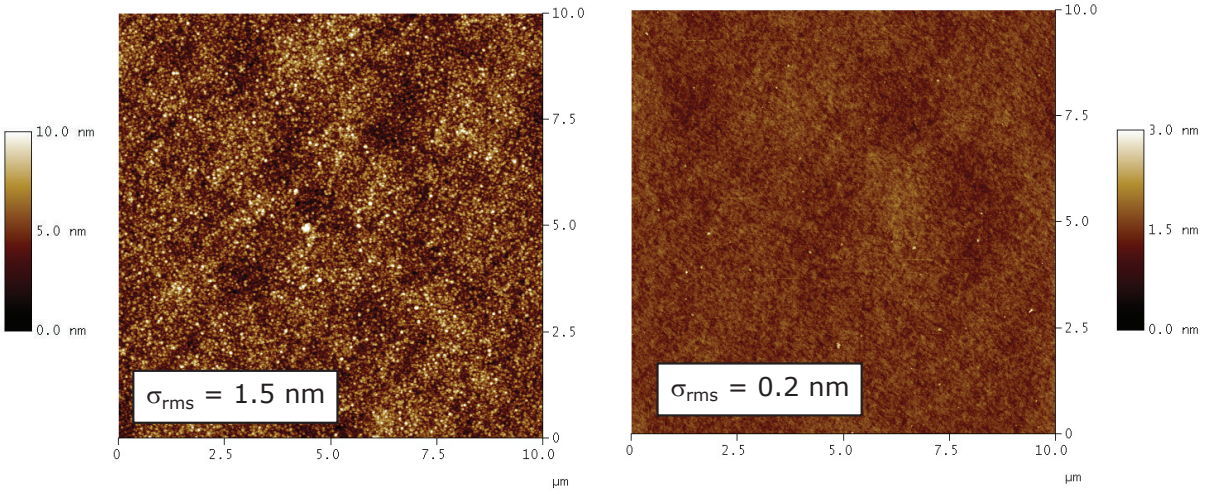

(beam splitter surfaces after coating) (coated surface after chemical mechanical polishing)

Figure 2. Images from atomic force microscopy (AFM) with a measurement size of 100 µm² after coating (left) and after chemical mechanical polishing of the coated surface (right).

Test samples and prisms were manufactured with strict requirements on surface flatness. This requirement was checked for all samples prior to bonding by Fizeau interferometry with a transmission plate with surface flatness better than $\lambda/20$. Exemplary results are presented for a round test substrate (fig. 3, left) and the bonding surface of prism A (fig. 3, right).

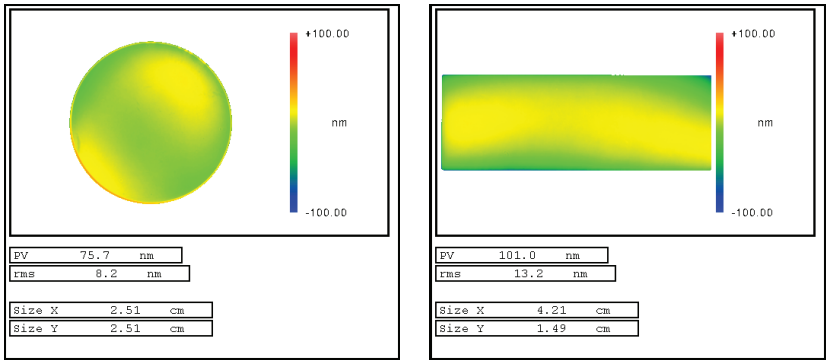

(test sample surface) (bonding surface of a prism)

Figure 3. Images from Fizeau interferometry of a test sample (left) and the bonding surface of a prism A (right).

3.2 Bonding process flow

For direct bonding, samples with the appropriate surface topography are cleaned thoroughly with ultrasonic assisted bath cleaning and spin cleaning. The cleaned samples are then plasma activated with nitrogen and

oxygen plasma to remove any organic residuals. Dangling bonds form on the surface during the plasma treatment. A subsequent water based spin cleaning step forms a hydrophilic surface. For pure SiO_2 surfaces as in our case, both surfaces to be bonded are then terminated by -OH groups. Two cleaned and activated samples are contacted to form a connection by weak atomic interactions. A heat treatment at moderate temperatures (below 300°C) enables a chemical reaction to form covalent bonds. The -OH groups are thought to react with each other under the formation of water.[5] Hence a strong Si-O-Si connection is formed between the surfaces.
As reported in section 2, we evaluated different materials as medium-index material, i.e. Si_3N_4 and Ta_2O_5. Besides the evaluation of their optical properties, we examined the influence on the bonding properties, namely on the mechanical bonding strength and the mechanical properties after cooling to cryogenic temperature (140 K). Therefore, we prepared test substrates (cylindrical glass samples with a diameter of 25 mm and a thickness of 6.35 mm) with and without coatings. The uncoated samples serve as a reference. The coatings were sputtered onto the test substrates. The substrates were then CM polished and tested for appropriate roughness (fig. 2) and flatness (fig. 3). Direct bonding was performed as described above. A representative image of a bonded pair of test substrates is shown in fig. 4.

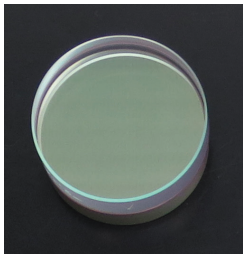

Figure 4. Example of a bonded test substrate, where one test cylinder was coated with a beamsplitter coating and CM polished afterwards. The coated cylinder was bonded to an uncoated cylinder.

3.3 Bonding Strength

The bonded cylindrical substrates were cut into pieces for a three-point-bending test ($5 \cdot 5 \cdot 12.7\,\mathrm{mm}^3$), with the bonding area parallel to the smallest plane. In this bending test, a force is applied parallel to the bonding plane. This results in tensile and compressive stresses at the bonding area. From the beam dimensions and the breaking force, the bonding strength is revealed, which corresponds to a bending strength. A part of the prepared beams were subjected to cryogenic temperatures within a cryostat setup. The samples were cooled to 140 K over a liquid nitrogen reservoir. The samples were hold at 140 K for two hours, before heating to room temperature again. These beams were then tested for bonding strength. The results of the test with Si_3N_4 and Ta_2O_5 as medium index material are shown in fig. 5. In this figure, the bonding strength of the directly bonded samples are compared to the bonding strength of adhesive bonded samples (dark grey box) and optically contacted samples (light grey box). The difference of the bonding strength of the samples tested after bonding with different medium index material is not significant (45-50 MPa, within the statistical deviation). The difference in the bonding strength of the coated samples after bonding and after cryogenic treatment is also within statistical deviation (45-60 MPa). The bonding strength of the coated and bonded samples is slightly reduced, compared to the bonding strength of the uncoated samples (80 MPa after bonding). Nevertheless, the bonding strength of the coated samples is in the range or slightly above the bonding strength of adhesive bonded samples.

3.4 Evaluation of Mechanical Stress

For testing mechanical stresses, that potentially occur during the bonding process, we performed polarimetry measurements on beams prepared from bonded cylinders. Polarimetry is able to reveal stresses, provided that they are constant along the irradiated volume of the material. Differences in surface flatness or coefficients of thermal expansions (CTE) within the coating may introduce bending stresses. Therefore, we irradiated beams, made from fused silica test structures shown in fig. 4, with linearly polarized light parallel to the bonding plane, to observe their stresses. The angle of rotation of the polarization plane corresponds to the mechanical stress.

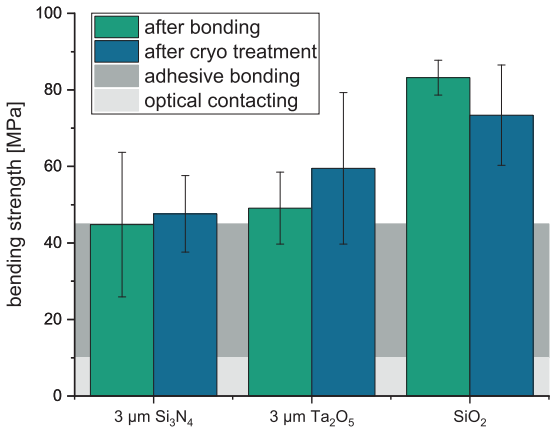

Figure 5. Bonding strength of test samples after bonding (green) and after cryogenic treatment (blue), compared to adhesive bonded samples (dark grey) and optically contacted samples (light grey). Coated samples with 4 µm coating thickness and either Si_3N_4 or Ta_2O_5 as medium index material are compared to an uncoated (pure fused silica) sample as reference.

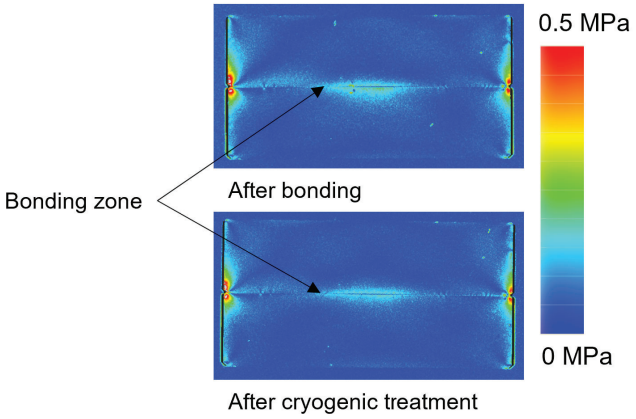

Figure 6. Representative polarimetry images of uncoated bonded samples after bonding (upper image) and after cryogenic treatment (lower image) with corresponding stresses in the bonding area. The bonding area is the line in the middle of the samples.

The exemplary results of the polarimetry measurements are shown in fig. 6. Here we performed polarimetry after bonding and after cryogenic treatment, again with a different coating composition (with Si_3N_4 or Ta_2O_5 as medium index material). The bonding area is visible as a line in the middle of the substrates. We compared the maximum achieved stress in the bonding area (table 2). The coating systems containing Si_3N_4 show slightly higher stresses (0.6 MPa) compared to Ta_2O_5 containing coatings (0.2 MPa). The mechanical stresses are below 1 MPa and are therefore uncritical for the optical and mechanical performance of the assembly.

4. MECHANICAL MOUNTING

To perform the mounting of the prism pairs, we evaluated different approaches. In the end, silicate bonding outperformed the other approaches.[4] Silicate bonding (also known as hydroxide catalysis bonding) is widely used for structural assembly in gravitational wave detectors, also in space.[8] An inorganic silicate solution is

Table 2. Maximum stress in the bonding area, revealed by polarimetry, in bonded (uncoated and coated with different medium index material) samples after bonding and after cryogenic treatment

sample	after bonding [MPa]	after cryogenic treatment [MPa]
Si_3N_4	0.6	0.6
Ta_2O_5	0.2	0.2
uncoated	0.1	0.1

applied onto one sample surface. Shortly afterwards, the second sample is placed onto the first sample and is let sit. A chemical reaction forms a silicate network between the bonding partners. We achieved the best bonding results, when bonding polished surfaces. The requirements on the surface quality are less strict compared to direct bonding ($\sigma_{rms} < 1$ nm; flatness better than 3 µm peak-to-valley). Since direct bonding resulted in a small vertical offset of the base plane of the prism pairs, these planes were ground and polished to form an uniform plane, as required for silicate bonding.
The three coated beam splitter prism pairs were bonded onto a triangular fused silica base plate to realize the vacuum gaps for the internal reflection. Special mechanical fixtures enable high precision alignment, to achieve the necessary optical performance. The successfully assembled beam splitter is presented in fig. 7. By three coordinate measurement we revealed an vacuum gap parallelism better than 0.05° (fulfilling the requirement of <0.1°).

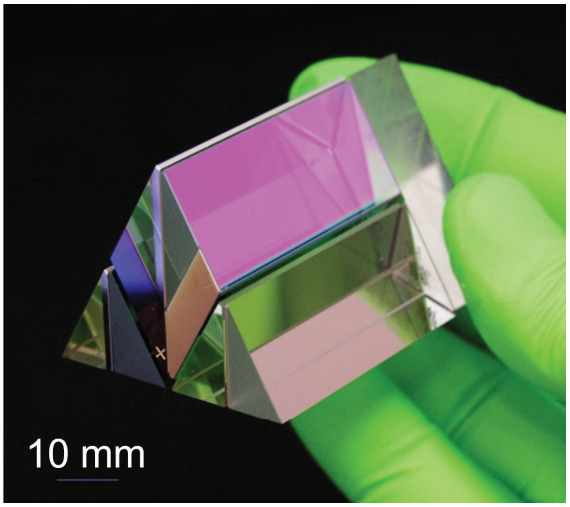

Figure 7. Successful assembly of an all-glass four channel beam splitter.

5. CONCLUSIONS AND OUTLOOK

We presented the successful manufacturing of a four-channel Kösters type beam splitter for use in space. We focussed on the results obtained for the different bonding technologies and especially their mechanical performance (bonding strength and mechanical stress). Plasma-activated bonded and coated surfaces have a high bonding strength (up to 50 MPa) and therefore are feasible for space applications. In addition, we observed only low mechanical stresses of the coated samples (maximum 0.6 MPa). Silicate bonding was successfully used to to achieve high precision bonding of the whole beam splitter assembly. The next steps are to perform further mechanical and climate testing. Furthermore, it is planned to evaluate the optical performance at cryogenic temperatures.

6. ACKNOWLEDGMENTS

We greatly acknowledge support by the industrial board of the research group (Forschergruppe "SpaceOptics"), especially Dr. Jochen Greiner from the Max Planck Institute for Extraterrestrial Physics, for countless hints and suggestions on coating realization and component manufacturing issues. We thank Britta Satzer, Uwe Lippmann from Fraunhofer Institute of Applied Optics and Precision Engineering (IOF) and Uwe Laux from Thüringer Landessternwarte Tautenburg for their support with the optical design. We thank Prof. Dr. Frank Schmidl, Faculty of Physics and Astronomy, Friedrich Schiller University Jena, Germany, and his team for performing laboratory tests at cryogenic conditions. We thank the group of Dr. Marcus Trost, IOF, for various AFM measurements. Gerd Harnisch, IOF, supported us with design of mechanical fixtures. Gilbert Leibeling, IOF, performed CM polishing and prism preparation. We thank Dr. Peter Munzert, IOF, for help and fruitful discussions on the coating design. We thank Christian Klose, IOF, for performing coordinate measurements and Karina Jorke, IOF, for performing bonding experiments. We are grateful for Dr. Felix Dreisow's support during the early phase of the project proposal. Last not least, we are very thankful for financial support by the European Social Fund and the Free State of Thuringia and for administrative support by the Thüringer Aufbaubank. This work was funded by the European Social Fund and the Free State of Thuringia, as "Forschergruppe SpaceOptics" (research group) under contract sign 2017 FGR 0071.

REFERENCES

[1] "Skyhopper mission." https://skyhopper.research.unimelb.edu.au/.

[2] Kösters, W., "Interferenzdoppelprisma fuer messzwecke," (1934). DE595211C.

[3] Greiner, J. and Laux, U., "A novel compact 4-channel beam splitter based on a kösters-type prism," *CEAS Space Journal* **14**, 253–260 (jan 2022).

[4] Rothhardt, C., Klose, S., Satzer, B., Schmidl, S., Grabowski, K., Birckigt, P., Hilpert, E., Lippmann, U., Schlegel, R., Shestaeva, S., Schwinde, S., and Risse, S., "Technical layout and fabrication of a compact all-glass four-channel beam splitter based on a kösters design," *CEAS Space Journal* **14**, 287–301 (apr 2022).

[5] Gösele, U. and Tong, Q.-Y., "SEMICONDUCTOR WAFER BONDING," *Annual Review of Materials Science* **28**, 215–241 (aug 1998).

[6] Rothhardt, C., Rothhardt, J., Klenke, A., Peschel, T., Eberhardt, R., Limpert, J., and Tünnermann, A., "BBO-sapphire sandwich structure for frequency conversion of high power lasers," *Optical Materials Express* **4**, 1092 (may 2014).

[7] Flügel-Paul, T., Rothhardt, C., Benkenstein, T., Grabowski, K., Risse, S., Eberhardt, R., Guldimann, B., and Zeitner, U. D., "All-dielectric prism-grating-prism component realized by direct hydrophilic bonding technology for optical applications in space," (jul 2019).

[8] Fitzsimons, E. D., Roberston, D. I., Ward, H., Killow, C. J., and Perreur-Llyod, M., "Mechanisation of precision placement and catalysis bonding of optical components," (sep 2017).